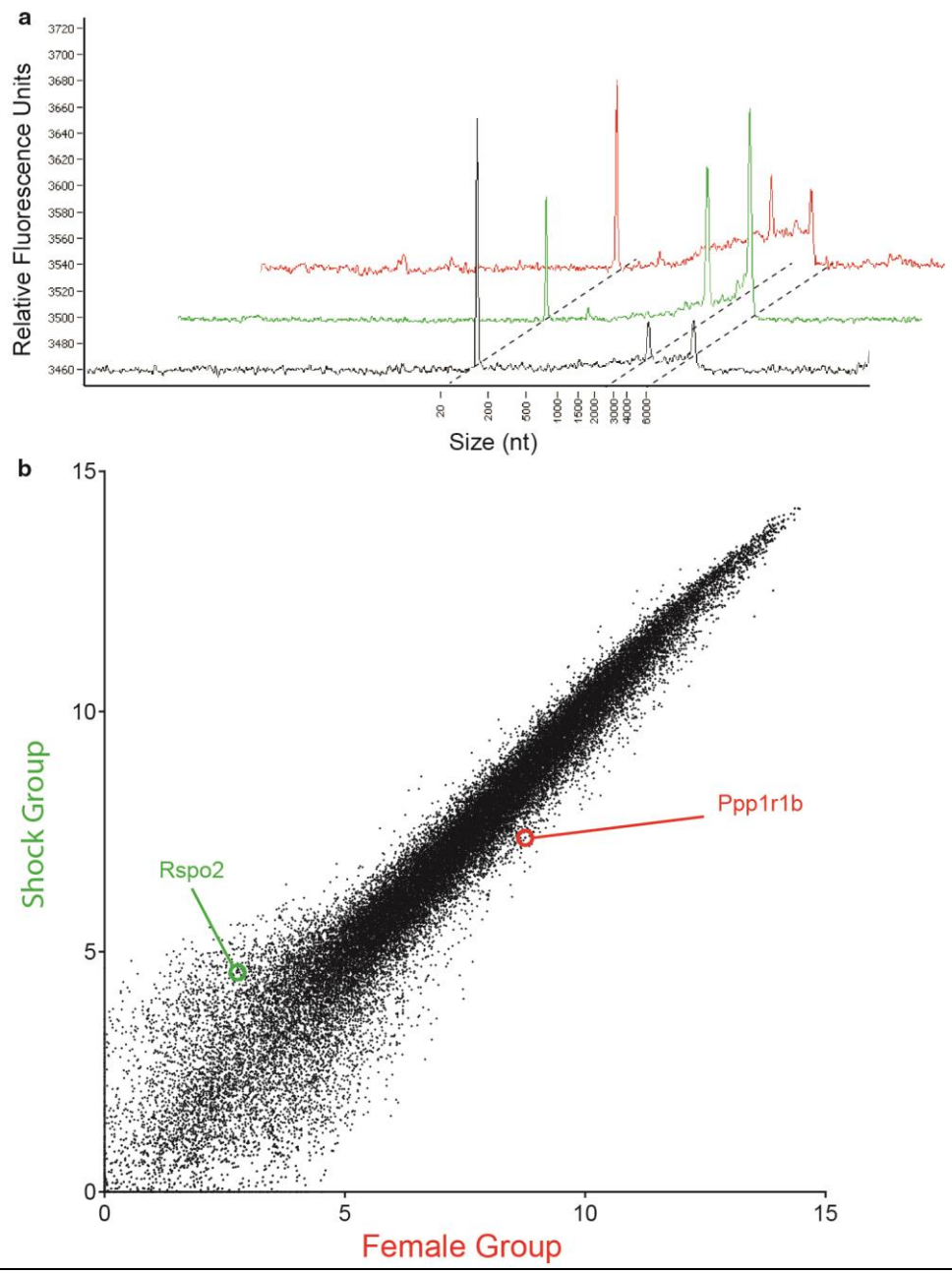

Supplementary Figure 1

RNA analysis of activity-dependent transcriptional profiles from BLA neurons.

a, Example bioanalyzer traces of RNA samples collected from footshock (green) (*n* = 3), female (red) (*n* = 3), on dox (black) group (*n* = 1). Bioanalyzer traces was used to test the quality of RNA sample for RNA microarray, the graph shows the fluorescence levels, which corresponds to RNA levels, of different RNA species of different size (nt). Bioanalyzer traces showed that footshock and female samples yielded RNA samples with RNA quality number (RQN) >6 (*n* = 6), while the on dox RNA sample RQN <4 (*n* = 1). Peaks at .02kb, 1.9kb and 4.7kb correspond to the marker, 18S rRNAs, and 28S rRNAs, respectively. b, Analysis of MAS5 normalized data of arrays from the footshock (*n* = 3) and female (*n* = 3) group.

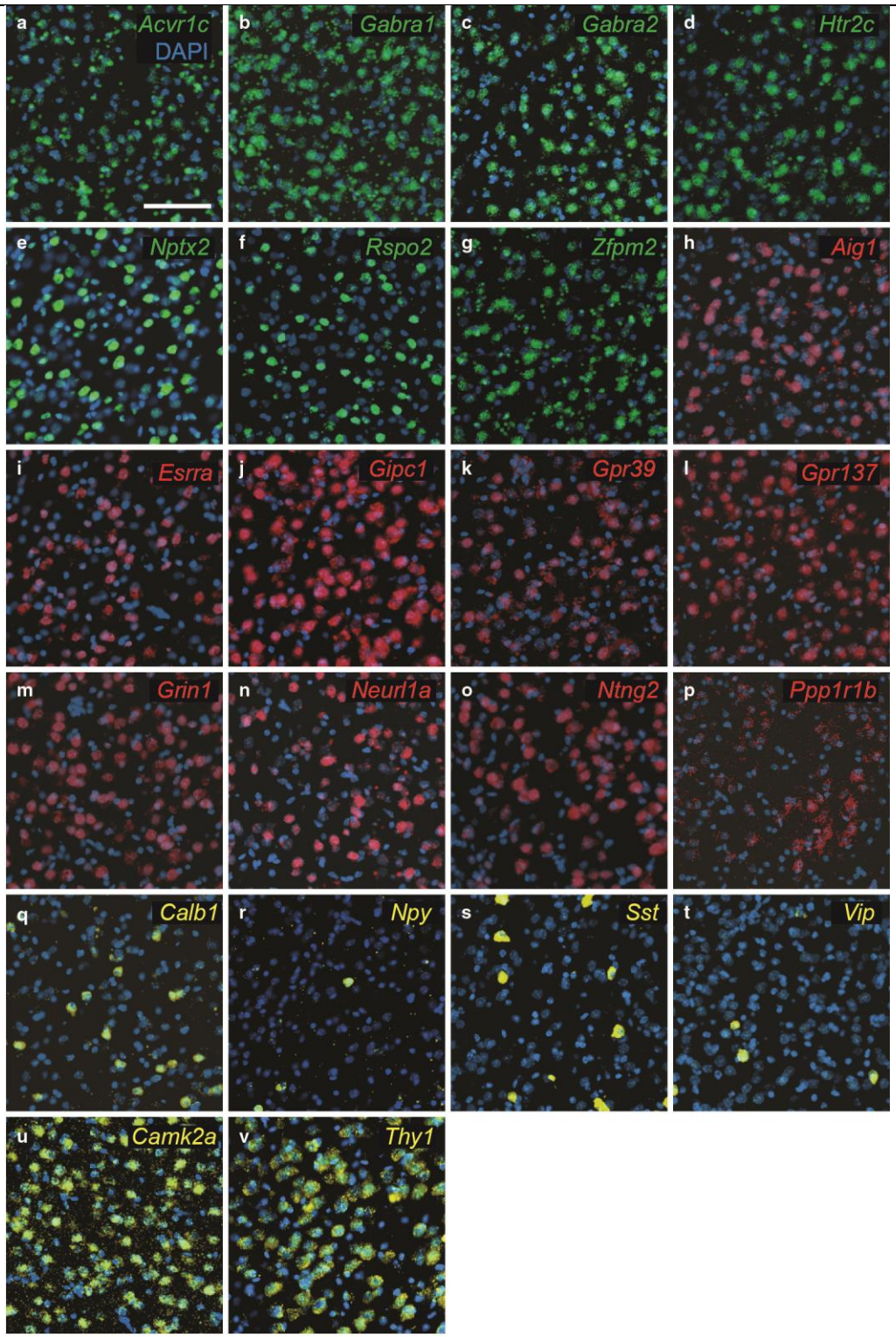

Supplementary Figure 2

In situ hybridization of candidate genetic markers of BLA neurons.

Gene expression of candidate genetic markers in the BLA using in situ hybridization. a-g, Genes that were enriched in the array of the footshock group (green). h-p, Genes that were enriched in the array of the female group (red). q-t, Positive control for interneurons

(yellow). u,v, Positive control for excitatory neurons (yellow). Micrographs represent FISH with the exception of *Ppp1r1b* (smFISH). a-v, nuclear marker, DAPI (blue). Scale bar 100µm.

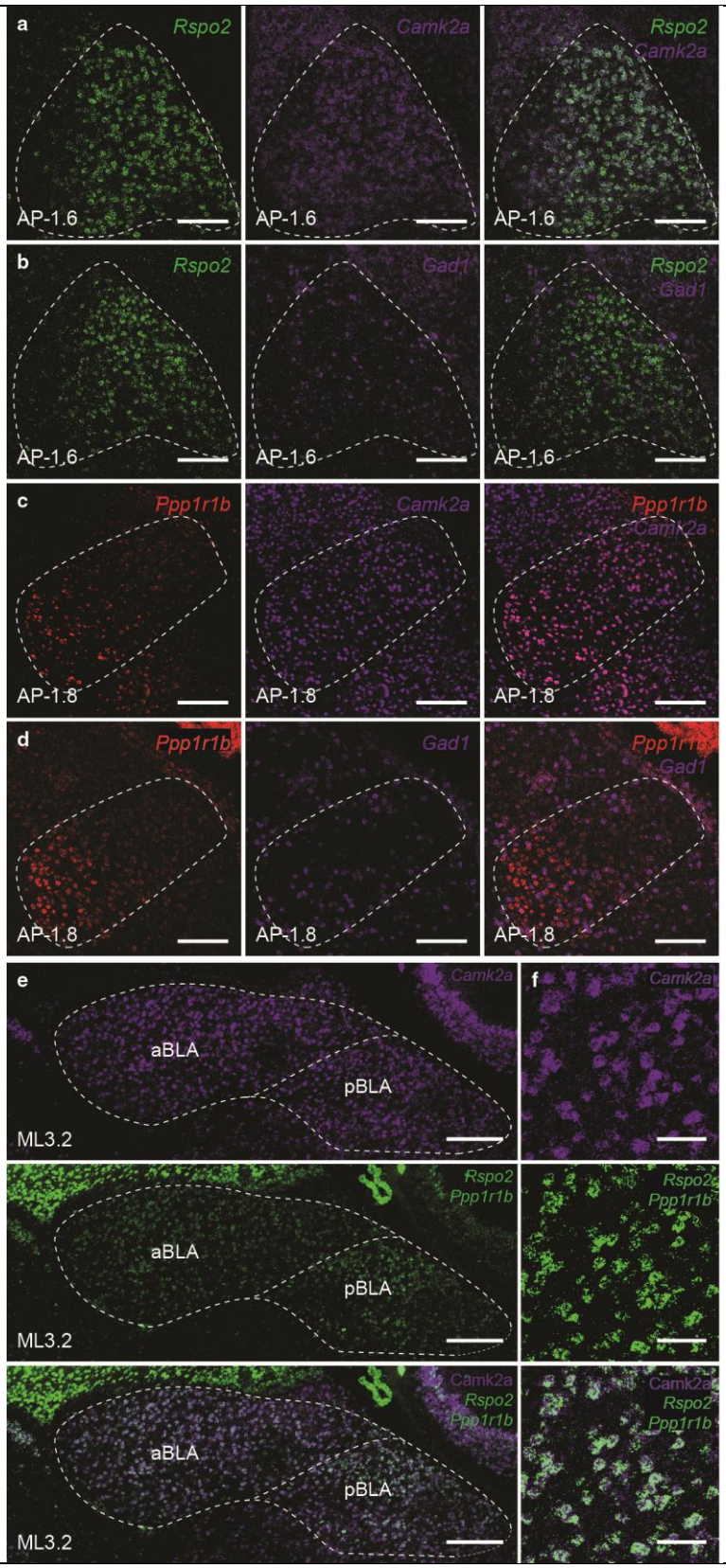

Supplementary Figure 3

***Rspo2*$^{+}$ and *Ppp1r1b*$^{+}$ BLA neurons collectively constitute all BLA pyramidal neurons.**

smFISH of *Rpso2*/*Camk2a* (a), *Rspo2*/*Gad1* (b), *Ppp1r1b*/*Camk2a* (c), *Ppp1r1b*/*Gad1* (d), coronal BLA, scale bar 200 µm. e, smFISH of *Rpso2*+*Ppp1r1b*/*Camk2a*, sagittal BLA, scale bar 250 µm. f, higher magnification expression of *Rpso2*+*Ppp1r1b*/*Camk2a*, scale bar 50µm.

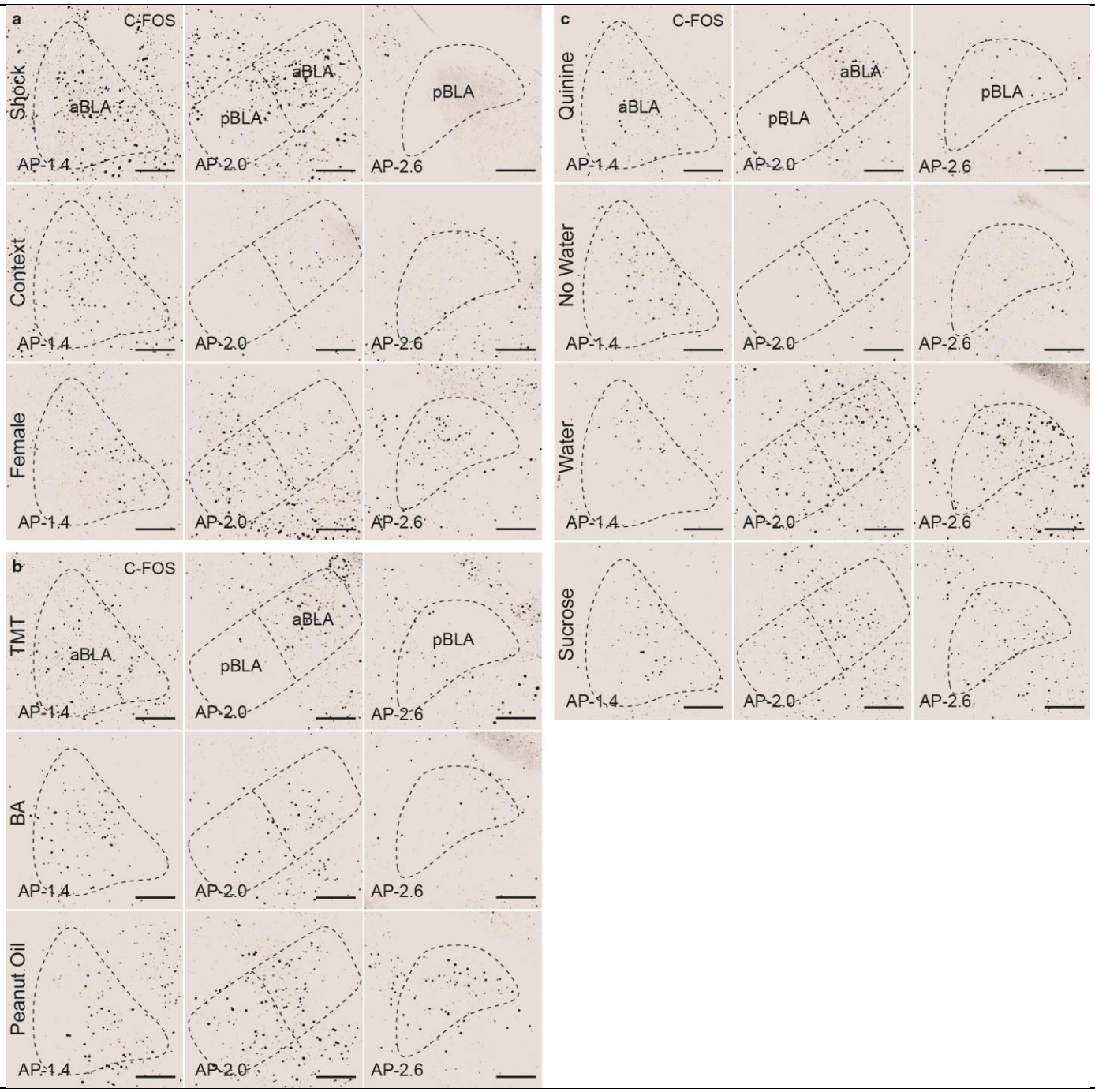

Supplementary Figure 4

Spatial distribution of c-Fos expression in the BLA in response to valence-specific stimuli.

c-Fos protein was visualized using IHC by an Alexa Fluor 555 secondary antibody. For improved graphical representation, images were inverted and saturation removed. a, c-Fos expression across the AP-axis of the BLA in response to shock, context, female. b, c-Fos expression across the AP-axis of the BLA in response to olfactory stimuli. c, c-Fos expression across the AP-axis of the BLA in response to gustatory stimuli. Scale bar 250µm.

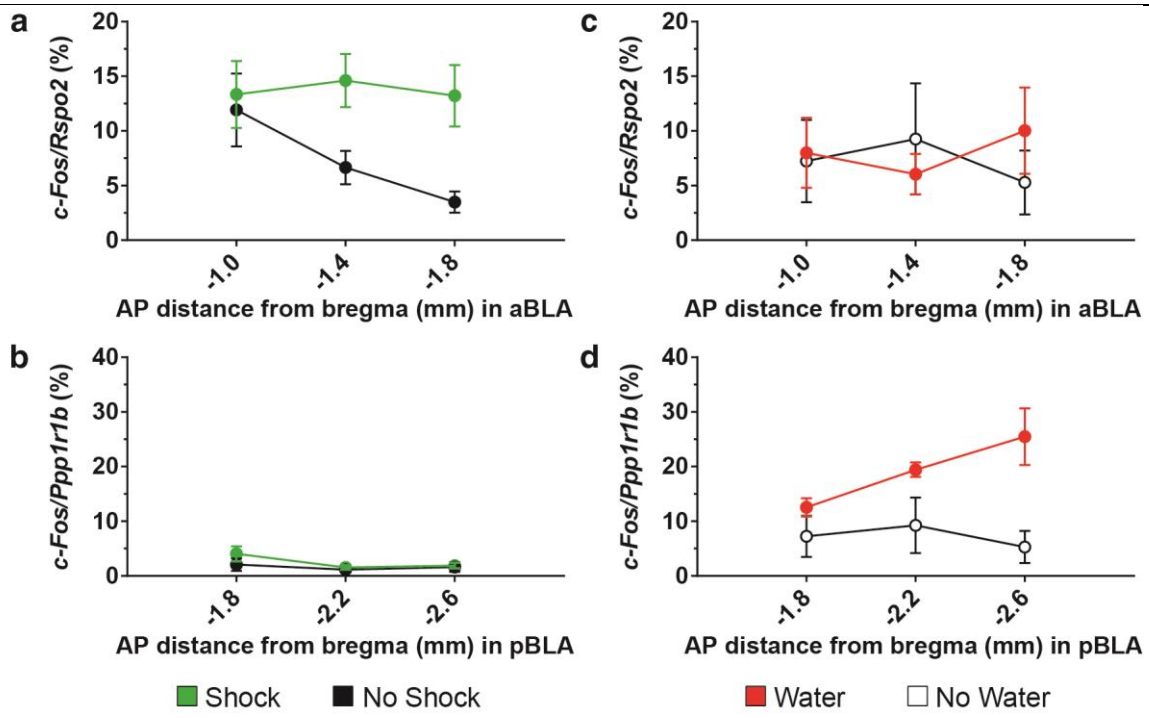

Supplementary Figure 5

Spatial distribution of *c-Fos* expression in *Rpso2*$^+$ or *Ppp1r1b*$^+$ BLA neurons in response to valence-specific stimuli.

Analysis from data found in Fig. 3g-j. *c-Fos* expression in *Rpso2*$^+$ (a) or *Ppp1r1b*$^+$ (b) BLA neurons across the AP-axis (mm distance from bregma) in response to shock or no shock. *c-Fos* expression in *Rpso2*$^+$ (c) or *Ppp1r1b*$^+$ (d) BLA neurons across the AP-axis in response to water or no water. Results show mean ± s.e.m (a-d).

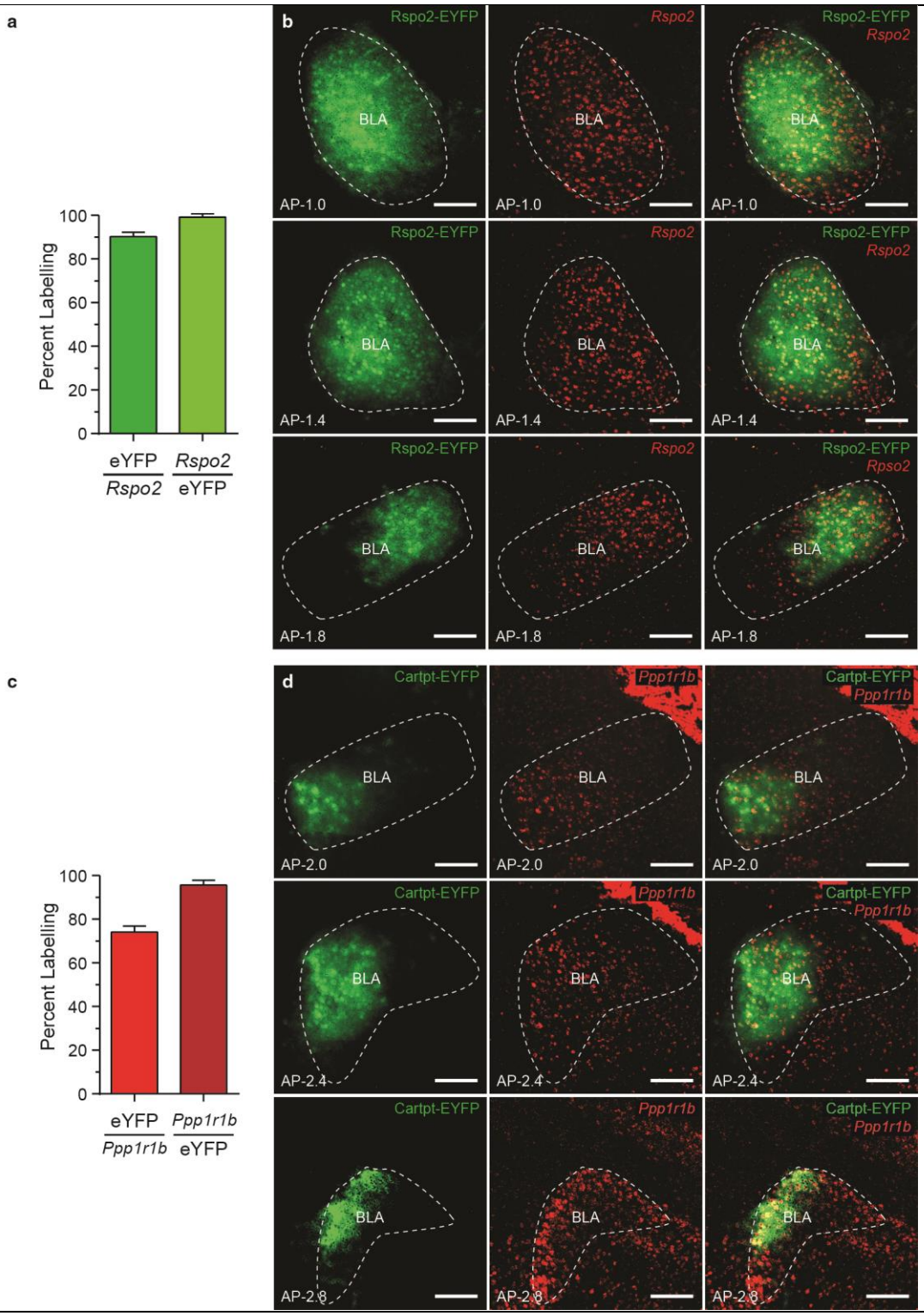

Supplementary Figure 6

Validation of Cre-driver mouse lines for targeting Rspo2$^+$ and Ppp1r1b$^+$ BLA neurons.

Rpso2-Cre and Cartpt-Cre mice were injected with a Cre-dependent eYFP virus into the BLA and smFISH was performed against *Rspo2* and *Ppp1r1b*, respectively. a, Quantification of the percentage of *Rpso2*$^+$ BLA neurons that express eYFP (eYFP/*Rspo2*) and

the percentage of eYFP$^+$ BLA neurons that express *Rspo2* (*Rpso2*/eYFP) (*n* = 4). b, eYFP (green) and *Rspo2* (red) expression in the BLA of virus injected Rspo2-Cre mice. c, Quantification of the percentage of *Ppp1r1b*$^+$ BLA neurons that express eYFP (eYFP/*Ppp1r1b*) and the percentage of eYFP$^+$ BLA neurons that express *Ppp1r1b* (*Ppp1r1b*/eYFP) (*n* = 4). d, eYFP (green) and *Ppp1r1b* (red) expression in the BLA of virus injected Cartpt-Cre mice. Though *Ppp1r1b* is endogenously expressed outside of the BLA, such as in the intercalated cell mass, choroid plexus, and striatum (Fig. 2c), Cre-dependent virus targeted in the Cartpt-Cre mice does not express in these off targeted cells. Fuzziness of the eYFP signal reflect the effects of the protease digestion step of the smFISH. Scale bar 250µm.

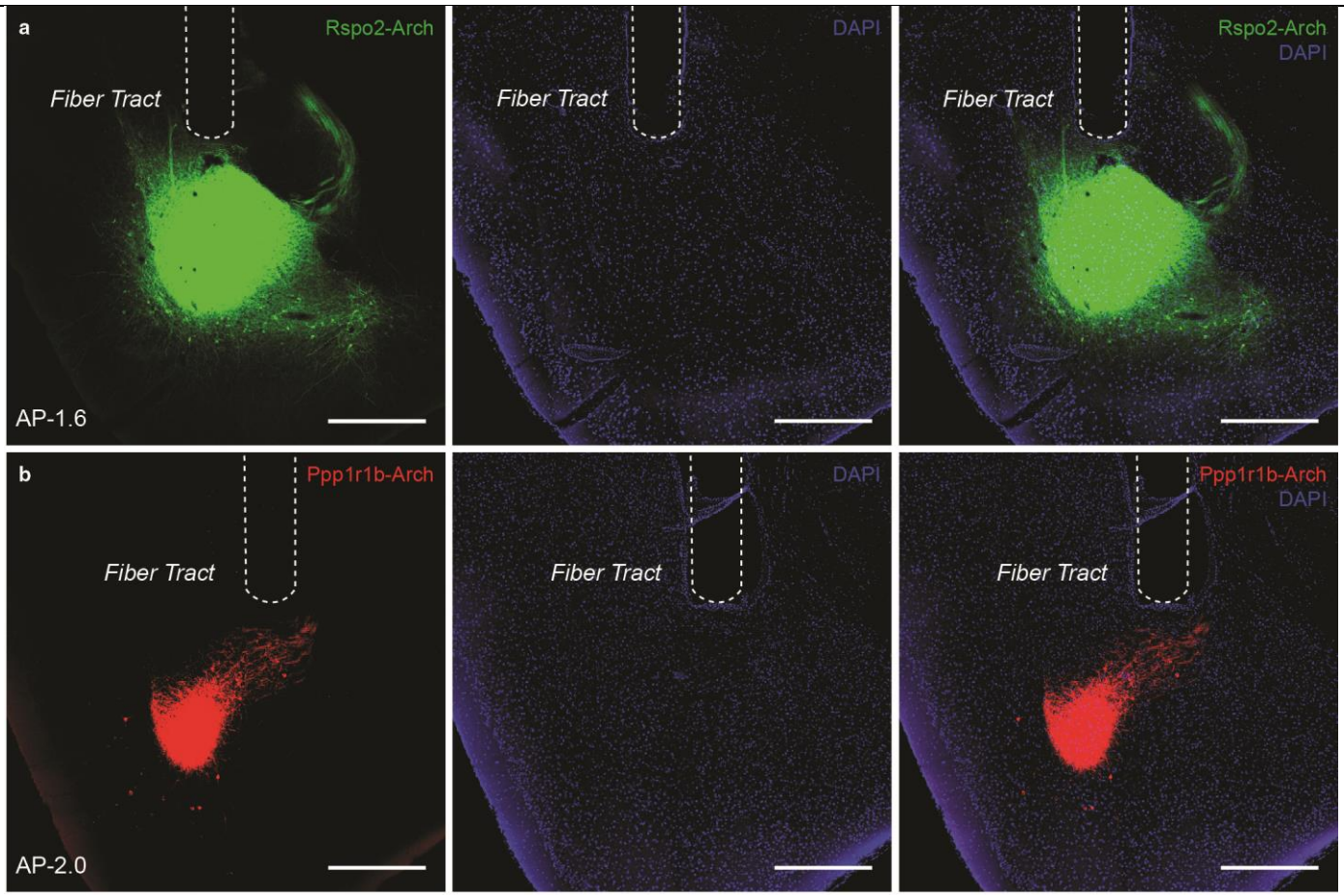

Supplementary Figure 7

Fiber placement for targeting Rspo2^{+} and Ppp1r1b^{+} BLA neurons.

Example of optic fiber placement in Rspo2-Arch (a) and Ppp1r1b-Arch (b) mice. Scale bar, 500µm.

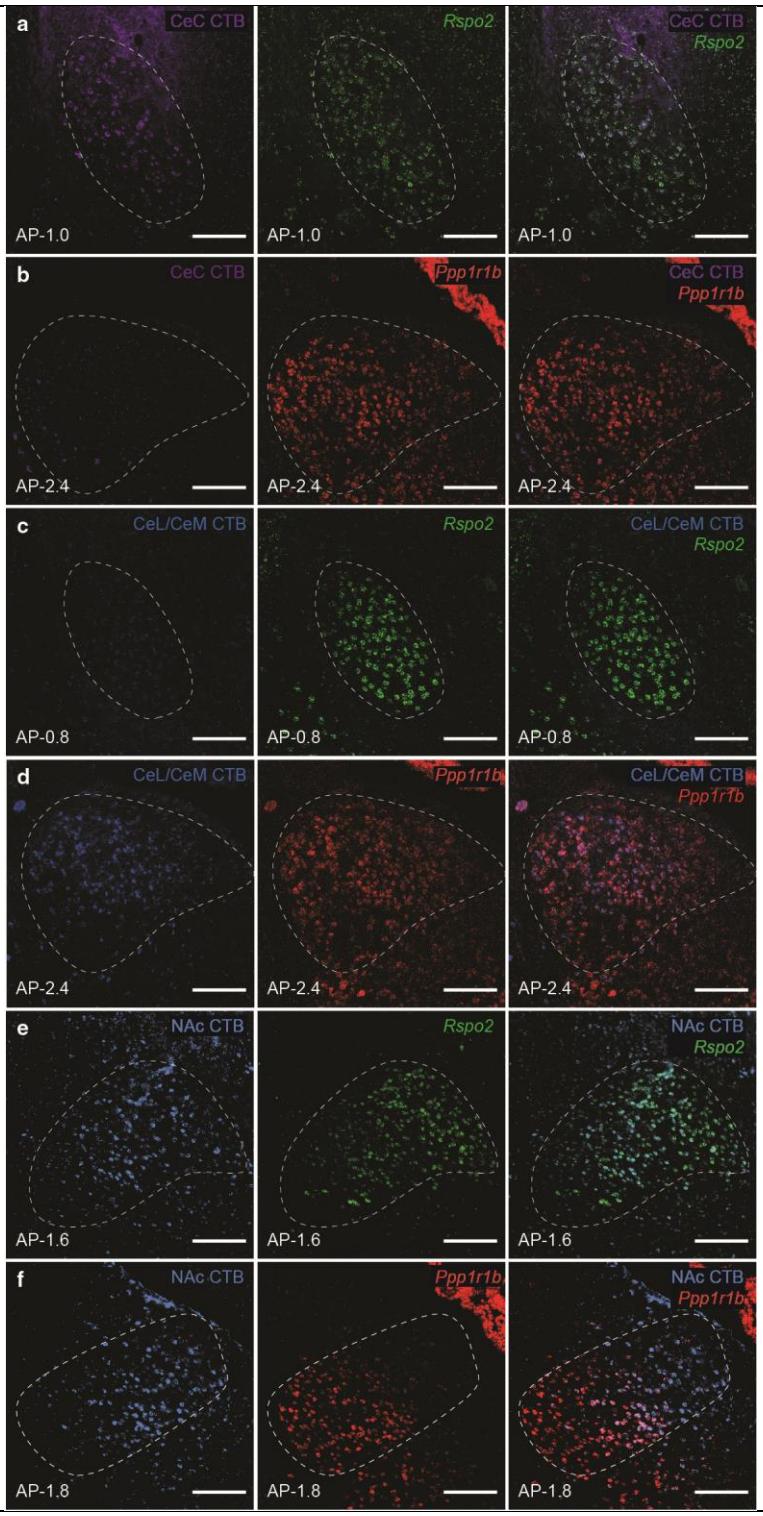

Supplementary Figure 8

Retrograde tracing from putative projection targets of *Rspo2*$^{+}$ and *Ppp1r1b*$^{+}$ BLA neurons.

smFISH of *Rspo2* and *Ppp1r1b* in CTB injected brains. *Rspo2* (a) and *Ppp1r1b* (b) expression in the BLA of CeC-CTB mice. *Rspo2* (c) and *Ppp1r1b* (d) expression in the BLA of CeL/M-CTB mice. *Rspo2* (e) and *Ppp1r1b* (f) expression in the BLA of NAc-CTB mice. Scale

bar 250µm.

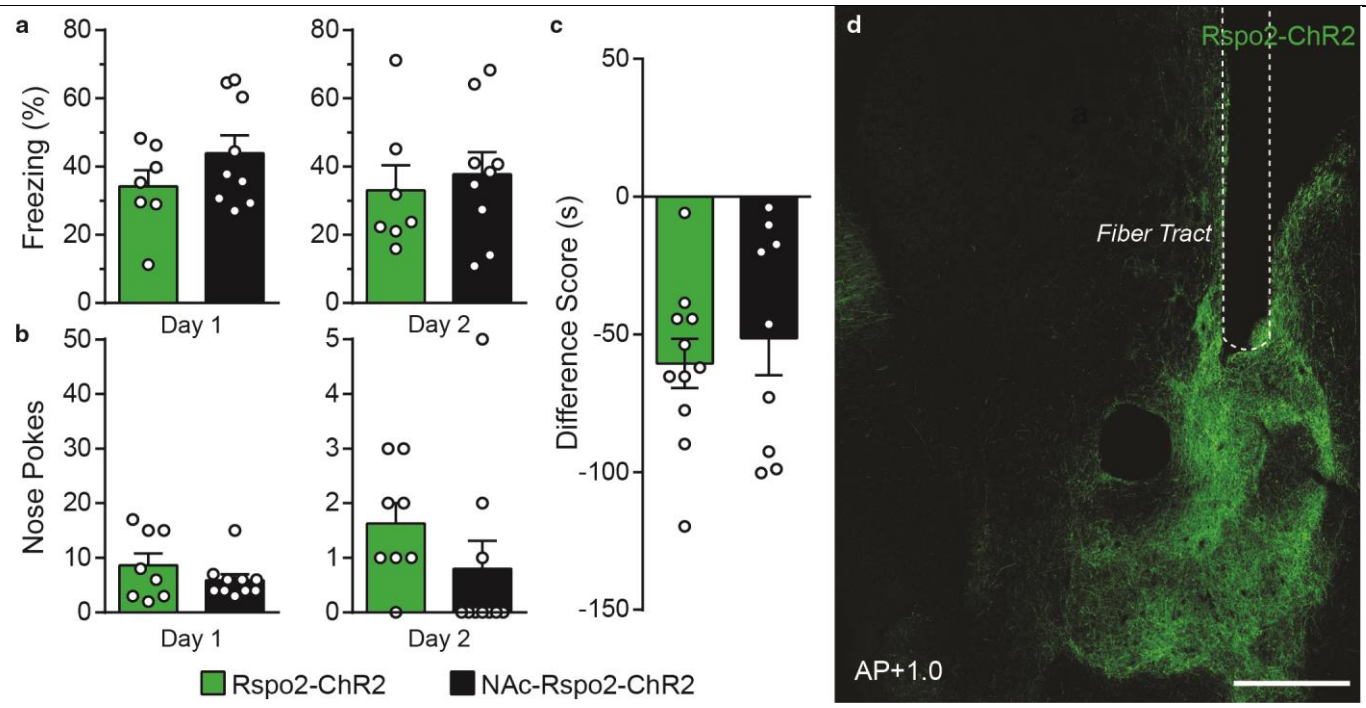

Supplementary Figure 9

Activation of NAc fibers of Rspo2^{+} BLA neurons elicits negative behaviors.

Optic fiber was unilaterally implanted above the NAc of Rspo-ChR2 mice (NAc Rpso2-ChR2). NAc Rspo2-ChR2 underwent behavioral assays. a, Optogenetic freezing test (*n* = 9). b, Optogenetic self-stimulation test (*n* = 11). c, Optogenetic place preference test (*n* = 9). Behavioral performance was compared against Rspo2-ChR2 (Fig. 4) using an unpaired *t-test*. No significant difference was observed across all assays. d, Optic fiber placement in the NAc of Rspo2-ChR2 mice. Significance for unpaired *t-test*, all comparison between ChR2 and eYFP groups not significant (N.S).

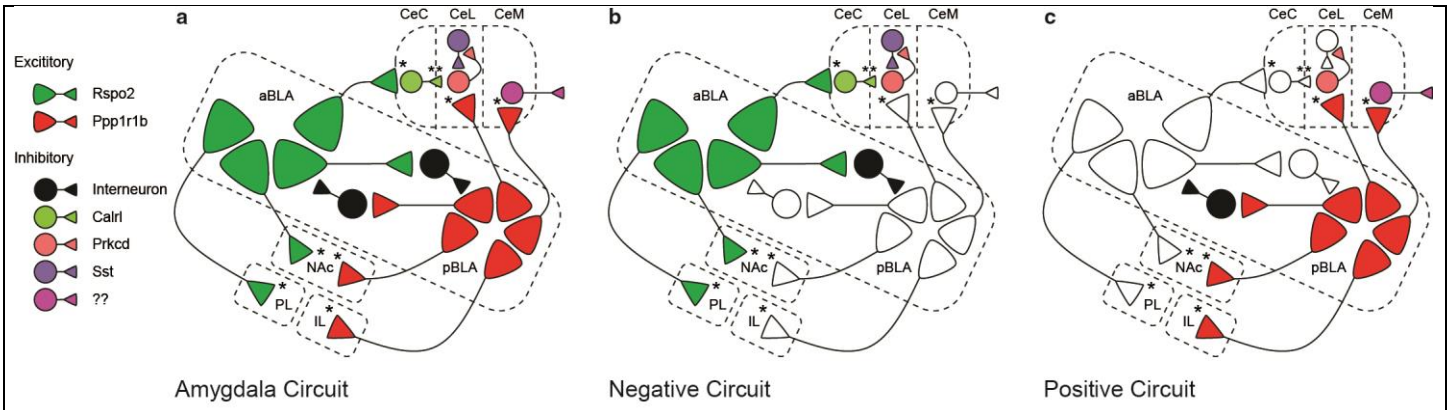

Supplementary Figure 10

| Circuit model of the BLA.

a, Anatomical connections of genetically identifiable populations of amygdala neurons. Projections identified, but cell-type unknown*, hypothetical**. b, The negative circuit of the amygdala (colored). CeC and PL projections are key distinguishing features of *Rspo2*$^{+}$ BLA neurons to *Ppp1r1b*$^{+}$ BLA neurons. *Rspo2*$^{+}$ BLA neurons project the CeC, but the genetic identity of the neurons that are innervated has yet to be identified; one possibility is CeL *Calcrl*$^{+}$ neurons. Nevertheless, if *Rspo2*$^{+}$ BLA neurons ultimately activate the effector neurons of freezing in the CeM, then an indirect route must be taken through the CeC and/or possibility the intercalated cell (not depicted). c, The positive circuit of the amygdala (colored). CeL, CeM, and IL projections are distinguishing features of *Ppp1r1b* $^{+}$ BLA neurons to *Rspo2*$^{+}$ BLA neurons. *Ppp1r1b* $^{+}$ BLA neurons send dense fibers to the CeL and CeM. Therefore, a population in the CeL and/or CeM may mediate appetitive behaviors.